Non-equilibrium Statistical Mechanics (Spring 2024)

Life at Low Reynolds Number: A Brief Review and Potential New Application

Abeer Karandikar
UG 24

Dr. Somendra M. Bhattacharjee

May 29, 2024

Abstract

In this report we take a look at E.M Purcell's scallop theorem which sates that propulsion through reciprocal strokes is not possible in low Reynold's number environments. We take a brief look at two proofs of the sane and move on to look at some interesting cases of the breakdown of the scallop theorem. In the final section, a candidate for an explanation for experimentally observed phenomena concerning nucleation near phase transitions in liquid crystal systems is given based on propulsion through shape deformation at low Reynold's number.

Low Reynolds Number

We start our analysis with the Navier-Stokes equation which is the standard starting in discussing fluid environments. The equation goes as follows:

$$\rho\left(\frac{\partial v}{\partial t} + (v \cdot \nabla)v\right) = -\nabla p + \eta \Delta v \tag{1}$$

Where v and p are the velocity and the pressure, ρ is the fluid density, η is the viscosity. The Reynolds number is a useful quantity which arises naturally when writing the Navier-Stokes in its non-dimensional form. Physically the Reynolds number represents the balance between the inertial versus viscous forces acting on a body in a fluid. On dividing 1 by a characteristic length L and a characteristic velocity V of the associated flow we define the Reynolds number (Re) as,

$$Re = \frac{VL\rho}{\eta} = \frac{VL}{\nu} \tag{2}$$

Where $\nu = \eta/\rho$ is the kinematic viscosity of the fluid (DeSimone et al., 2008). Here, we restrict ourselves to the low Reynolds number regime. This is occupied by microorganisms living usually in aqueous environments. To get an idea of what low Reynolds number might look like consider the following example: for a person swimming in a fluid medium a low Reynolds number environment would be experienced by swimming through hot roofing tar. Such an environment gives rise to very peculiar phenomena which we will look at in the following sections.

The Scallop Theorem

In the seminal 1976 paper, Purcell (2014) first gave the statement of the scallop theorem as: A swimmer at low Reynolds number cannot swim using *reciprocal stroke*. A swimming stroke is said to reciprocal when it is symmetric when viewed forwards and backwards in time. The theorem is called the scallop theorem because a scallop uses such reciprocal strokes to swim in water. A scallop in water is able to exert thrust on the water and thus propel itself. But, in a low Reynolds number environment a scallop cannot swim at all. Let us now take a brief look at mathematical proofs for the scallop theorem.

A look at microscopic scallops

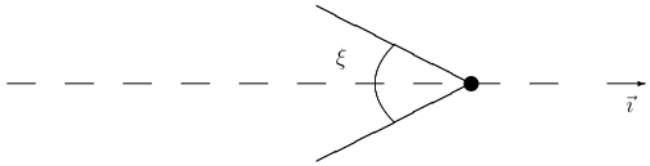

Figure 1: Schematic diagram of a micro-scallop. Image source: DeSimone et al. (2008), *Biological Fluid Dynamics: Swimming at low Reynolds numbers.*

We first look at the specific case of a scallop or more generally a single-hinged swimmer, the only possible stroke for such a swimmer is opening and closing the hinge. let x be the position of the hinge and ζ be the angle made between the opening of the two valves. The viscous force is directly proportional to the velocity of the boundary of the valve.

$$F_v = C_x(x,\zeta)\dot{x} + C_\zeta(x,\zeta)\dot{\zeta} = 0$$

The coefficients C_x and C_ζ depend on the shape of the scallop. The equation can be set due to the self-propulsion constraint (Morandotti, 2011). Let,

$$\phi(\zeta) := \int_0^\zeta -\left(\frac{C_\zeta(s)}{C_x(s)}\right) ds$$

The displacement in a stroke will be obtained by integrating over the period of stroke.

$$\Delta x = \int_0^T \dot{x}dt = -\int_0^T \frac{C_\zeta(\zeta(t))}{C_x(\zeta(t))}\dot{\zeta}(t)dt$$

$$= \int_0^T \frac{d}{dt}\phi(\zeta)dt = \phi(\zeta(T)) - \phi(\zeta(0))$$

From the definition of a reciprocal stroke we know that $\zeta(T) = \zeta(0)$
thus over one stroke, $\Delta x = 0$. Hence a scallop cannot move in a low Reynolds number environment.

Coordinate based approach for swimming by surface deformations

This proof of the scallop theorem is given by Ishimoto and Yamada (2012). Unlike the previous section where specifically single-hinged swimmers were considered, in this section any arbitrary swimmer swimming using surface deformations is considered. Here, a brief walk-through of the same is presented. To start a *virtual swimmer* is defined. This deforms

in exactly the same way as the real swimmer except it is considered sans the fluid surrounding. Thus, the *virtual swimmer* conserves the total momentum as well as angular momentum, both are assumed to be zero. The coordinates attached to the centre of mass of the virtual swimmer are called the *vacuum coordinates*.

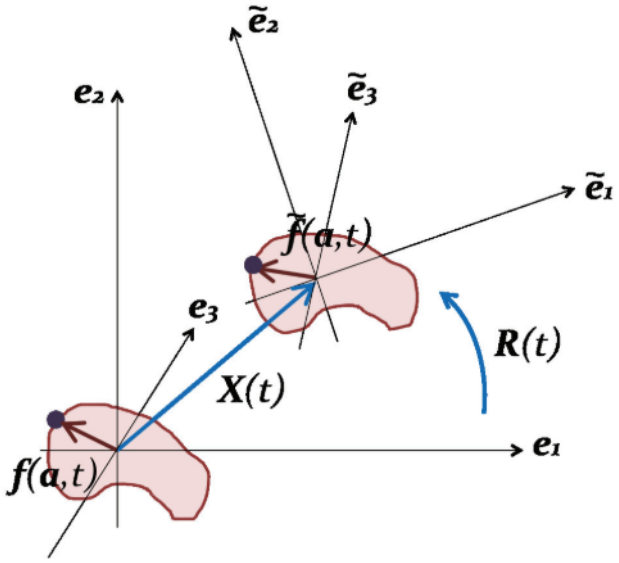

Figure 2: The vacuum coordiates $\{\tilde{e_i}\}$ the body coordinates $\{e_i\}$. Image source: Ishimoto and Yamada (2012), *A coordinate-based proof of the scallop theorem*

The *vacuum coordinates* are defined as the coordinates attached to the real swimmer. The two coordinates are related through an affine transformation. The motion of the swimmer can be described using the orthonormal basis of the *vacuum coordinates* as $\mathbf{e_i}$ where $i = 1, 2, 3$ by writing the lagrangian particle of the virtual swimmer as,

$$\mathbf{f}(\mathbf{a}, t) = \sum_i f_i(\mathbf{a}, t)\mathbf{e_i}$$

This in turn allows us to define the velocity of surface deformation as,

$$\mathbf{u}' = \sum_i \frac{\partial f_i}{\partial t}\mathbf{e_i}$$

Along with deforming the real swimmer also undergoes rotation and translation thus, we define $\mathbf{X}(t)$ as the centre of mass of the real swimmer and $\mathbf{U}(t) = \dot{\mathbf{X}}(t)$ is the velocity of translation of the real swimmer. The lagrangian particle for the real swimmer is given as,

$$\bar{\mathbf{f}}(\mathbf{a}, t) = \mathbf{R}(t) \cdot \mathbf{f}(\mathbf{a}, t) \implies \bar{f}_i = R_{ij} f_j$$

Where, $\mathbf{R}(t)$ is a rotation matrix with $\mathbf{R}(0) = \mathbf{I}$
The rotational velocity is defined as,

$$\frac{d\mathbf{R}(t)}{dt} = \mathbf{B}(t) \cdot \mathbf{R}(t) = \mathbf{R}(t) \cdot \mathbf{A}(t) = \mathbf{\Omega} \times \mathbf{R}(t) \tag{3}$$

Where, $\mathbf{A}(t)$ and $\mathbf{B}(t)$ are skew symmetrical matrices. Physically, $\mathbf{A}(t)$ is a part of the vector potential used by Shapere and Wilczek (1989) to describe the motion of a swimmer at low Reynold's number. Thus, the total surface velocity is defined as,

$$\mathbf{u} = \mathbf{U} + \frac{\partial \bar{\mathbf{f}}}{\partial t} = \mathbf{U} + \mathbf{\Omega} \times \bar{\mathbf{f}} + \bar{\mathbf{u}'} \tag{4}$$

Now, we can get to writing the incompressible Navier-Stokes equation for governing the fluid the real swimmer swims in,

$$\nabla \cdot \mathbf{\Pi} = R_\omega \frac{\partial \mathbf{v}}{\partial t} + Re(\mathbf{v} \cdot \nabla)\mathbf{v} \tag{5}$$

$$\nabla \cdot \mathbf{v} = 0 \tag{6}$$

Here, $\mathbf{\Pi}$ is the stress tensor given as,

$$\mathbf{\Pi} = -p\mathbf{1} + (\nabla \mathbf{v} + (\nabla \mathbf{v})^T) \tag{7}$$

The two non-dimensional here are of interest to us. R_ω and Re are the oscillatory Reynold's number and the Reynold's number respectively. The oscillatory Reynold's number is given by the product of the Reynold's number with another non-dimensional number, the Strouthal number: $St = L\omega/V$. L, V, ω are the characteristic length, velocity and frequency of the fluid motion respectively. The boundary conditions are as follows:

1. $\mathbf{v}$ coincides with the total surface velocity of the real swimmer $\mathbf{u}$ at the surface
2. $\mathbf{v} \longrightarrow 0$ at infinity.

Let, $\mathbf{F}$ be the nondimensinalised force and $\mathbf{T}$ be the nondimensionalised torque acting on the real swimmer. This if done as $\mathbf{F}_{dim} = \mu L V \mathbf{F}_{\mathbf{non-dim}}$.If $\bar{\mathbf{I}}$ is the moment of inertia tensor of the real swimmer we can write,

$$R_S \frac{d}{dt} \begin{pmatrix} \mathbf{U} \\ \bar{\mathbf{I}} \cdot \Omega \end{pmatrix} = \begin{pmatrix} \mathbf{F} \\ \mathbf{T} \end{pmatrix} \tag{8}$$

R_S is a nondimensional number called the Stokes number. given as

$$R_S = \frac{\rho_M L^2 \omega}{\mu}$$

Where, ρ_M is the mean density of the swimmer. The regime we are interested in implies, Re, R_ω, $R_S << 1$ The expressions for the velocity $\mathbf{U}$ and the angular velocity $\mathbf{\Omega}$ can be derived using the method used by Stone and Samuel (1996) from the following:

$$\int_{\tilde{S}} d\tilde{S}\mathbf{n}\cdot\mathbf{\Pi}\cdot\hat{\mathbf{u}} = \int_{\tilde{S}} d\tilde{S}\mathbf{n}\cdot\mathbf{\Pi}\cdot\mathbf{u} \tag{9}$$

$\tilde{S}$ and $d\tilde{s}$ represent the surface and surface element of the real swimmer while S and dS represent those for the virtual swimmer. $\hat{\mathbf{u}}$ is another solution to the Stokes equation with the same shape $\tilde{S}$. The solution $\hat{\mathbf{u}}$ is taken to satisfy the following boundary condition at the surface of the swimmer,

$$\hat{\mathbf{u}} = \hat{\mathbf{U}} + \hat{\mathbf{\Omega}}\times\hat{\mathbf{f}} \tag{10}$$

Let, $\tilde{\mathbf{\Sigma}_\mathbf{T}}$ and $\tilde{\mathbf{\Sigma}_\mathbf{R}}$ be rank three tensors which are dependent on the direction of the body coordinates, $\tilde{\mathbf{e}}_i$. Then the stress tensor of the swimmer is given as,

$$\hat{\mathbf{\Pi}} = \tilde{\mathbf{\Sigma}_\mathbf{T}}\cdot\hat{\mathbf{U}} + \tilde{\mathbf{\Sigma}_\mathbf{R}}\cdot\hat{\mathbf{\Omega}} \tag{11}$$

By substituming 10 and 11 in 9

$$\begin{pmatrix}\mathbf{F}\\ \mathbf{T}\end{pmatrix}\cdot\begin{pmatrix}\hat{\mathbf{U}}\\ \hat{\mathbf{\Omega}}\end{pmatrix} = \int_{\tilde{S}} d\tilde{S}\begin{pmatrix}(\mathbf{n}\cdot\tilde{\mathbf{\Sigma}_\mathbf{T}})^T\cdot\mathbf{u}\\ (\mathbf{n}\cdot\tilde{\mathbf{\Sigma}_\mathbf{R}})^T\cdot\mathbf{u}\end{pmatrix}\cdot\begin{pmatrix}\hat{\mathbf{U}}\\ \hat{\mathbf{\Omega}}\end{pmatrix} \tag{12}$$

$$\tilde{\kappa} = \begin{pmatrix}\tilde{\mathbf{K}}_T & \tilde{\mathbf{K}}_C^T\\ \tilde{\mathbf{K}}_C & \tilde{\mathbf{K}}_R\end{pmatrix} = \int_{\tilde{S}} d\tilde{S}\begin{pmatrix}\mathbf{n}\cdot\tilde{\mathbf{\Sigma}}_T & \mathbf{n}\cdot\tilde{\mathbf{\Sigma}}_R\\ \tilde{\mathbf{f}}\times(\mathbf{n}\cdot\tilde{\mathbf{\Sigma}}_T) & \tilde{\mathbf{f}}\times(\mathbf{n}\cdot\tilde{\mathbf{\Sigma}}_R)\end{pmatrix} \tag{13}$$

$$\begin{pmatrix}\mathbf{F}\\ \mathbf{T}\end{pmatrix} = \tilde{\kappa}\cdot\begin{pmatrix}\mathbf{U}\\ \mathbf{\Omega}\end{pmatrix} + \int_{\tilde{S}} d\tilde{S}\begin{pmatrix}(\mathbf{n}\cdot\tilde{\mathbf{\Sigma}_\mathbf{T}})^T\cdot\mathbf{u}'\\ (\mathbf{n}\cdot\tilde{\mathbf{\Sigma}_\mathbf{R}})^T\cdot\mathbf{u}'\end{pmatrix} \tag{14}$$

Taking a negligible Stokes number R_S in 8 we obtain:

$$\begin{pmatrix}\mathbf{F}_{TR}\\ \mathbf{T}_{TR}\end{pmatrix} + \begin{pmatrix}\mathbf{F}_D\\ \mathbf{T}_D\end{pmatrix} = 0 \tag{15}$$

This leads to,

$$\begin{pmatrix}\mathbf{F}_{TR}\\ \mathbf{T}_{TR}\end{pmatrix} = \tilde{\kappa}\cdot\begin{pmatrix}\mathbf{U}\\ \mathbf{\Omega}\end{pmatrix} \text{ and } \begin{pmatrix}\mathbf{F}_D\\ \mathbf{T}_D\end{pmatrix} = \int_{\tilde{S}} d\tilde{S}\begin{pmatrix}(\mathbf{n}\cdot\tilde{\mathbf{\Sigma}_\mathbf{T}})^T\cdot\mathbf{u}\\ (\mathbf{n}\cdot\tilde{\mathbf{\Sigma}_\mathbf{R}})^T\cdot\mathbf{u}\end{pmatrix} \tag{16}$$

$\mathbf{F}_{TR}$ and $\mathbf{T}_{TR}$ are the external force and torque due to the translation and rotation of the real swimmer in the fluid. $\mathbf{F}_D$ and $\mathbf{T}_D$ are the force and torque arising due to the deformation of the real swimmer. In 15 the total force is taken into account thus the effects of gravitation and buoyancy need to be taken into account. The rank three tensors $\tilde{\mathbf{\Sigma}}_T$ and $\tilde{\mathbf{\Sigma}}_R$ and the

resistive tensor $\tilde{\kappa}$ of the real swimmer only depend on the shape of the surface of the real swimmer $\tilde{\mathbf{f}}(t)$. We are looking at the scallop theorem by studying the surface deformations of the *virtual swimmer* using the *vacuum coordinates*,

$$\kappa \cdot \mathscr{R}^{-1} \cdot \begin{pmatrix} \mathbf{U} \\ \mathbf{\Omega} \end{pmatrix} + \int_S dS \begin{pmatrix} (\mathbf{n} \cdot \mathbf{\Sigma_T})^T \cdot \mathbf{u}' \\ (\mathbf{n} \cdot \mathbf{\Sigma_R})^T \cdot \mathbf{u}' \end{pmatrix} \tag{17}$$

Where, $\mathscr{R}$ is defined as 6×6

$$\mathscr{R} = \begin{pmatrix} \mathbf{R} & 0 \\ 0 & \mathbf{R} \end{pmatrix} \tag{18}$$

The proof of the scallop theorem can now be done. We will use 3 and 17. Consider a swimmer going through a reciprocal swimming stroke. The stroke is defined for the *virtual swimmer*, it goes starts the stroke at $t = 0$ and ends at $t = T$. $g(t)$ is a continuous function such that,

$$\mathbf{f}(t) = \mathbf{Q}(t) \cdot \mathbf{f}(g(t)) \text{ and } g(0) = g(T) = 0$$

Where, $\mathbf{Q}(t) \in SO(3)$ is a 3-dimensional rotation matrix. $g(t)$ is assumed to be smooth except at a finite number of points. The virtual swimmer is defined such that the total angular momentum is conserved therefore we get,

$$\int \rho_m \mathbf{Q}\mathbf{f}(\mathbf{a}, g(t)) \times \frac{\partial \mathbf{Q} \cdot \mathbf{f}(\mathbf{a}, g(t))}{\partial t} d\mathbf{a} = \mathbf{0} \tag{19}$$

$$\frac{\partial \mathbf{Q} \cdot \mathbf{f}(\mathbf{a}, g(t))}{\partial t} = \mathbf{\Omega}^Q \times \mathbf{f}(\mathbf{a}, t) + \frac{dg}{dt} \mathbf{Q} \cdot \frac{\partial \mathbf{f}}{\partial t} \tag{20}$$

Let, the angular velocity vector ($\mathbf{\Omega}^Q$) be defined as,

$$\frac{d\mathbf{Q}}{dt} = \mathbf{\Omega}^Q \times \mathbf{Q} \implies \Omega_i^Q = -\epsilon_{ijk} \left(\frac{d\mathbf{Q}}{dt} \cdot \mathbf{Q}^{-1} \right)_{jk}$$

The contribution from the second term in 20 in 19 vanishes as substituting only the second term we get,

$$\frac{dg}{dt} \mathbf{Q}(t) \cdot \int \rho_m \mathbf{f}(\mathbf{a}, g(t)) \times \frac{\partial \mathbf{f}}{\partial t} d\mathbf{a} = 0 \tag{21}$$

as the initial angular momentum is conserved, we get,

$$\int \rho_m \mathbf{f}(\mathbf{a}, t) \times (\mathbf{\Omega}^Q(t) \times \mathbf{f}(\mathbf{a}, t)) d\mathbf{a} = \mathbf{I}(t) \cdot \omega^Q(t) = 0 \tag{22}$$

$\mathbf{I}$ is the moment of inertia tensor for the *virtual swimmer*. We also have $\mathbf{\Omega}^Q(t) = 0$ then, using $\mathbf{Q}(0) = 1$ we get $\mathbf{Q}(t) = \mathbf{1}$. Wile looking at reciprocal strokes we have that the position

and direction of the real swimmer at $t = 0$ and ant $t = T$ must coincide. In such a case the surrounding fluid obeys the steady Stokes equation. 17 reduces to,

$$\begin{pmatrix} \mathbf{U} \\ \mathbf{\Omega} \end{pmatrix} = -\mathscr{R} \cdot \mathscr{M} \cdot \int_S dS \begin{pmatrix} (\mathbf{n} \cdot \sigma_{\mathbf{T}})^T \cdot \mathbf{u}' \\ (\mathbf{n} \cdot \sigma_{\mathbf{R}})^T \cdot \mathbf{u}' \end{pmatrix} \tag{23}$$

The tensor $\mathscr{M}$ is the mobility tensor defined as the inverse of the resistive tensor κ.

$$\begin{pmatrix} \mathbf{U}(t) \\ \mathbf{\Omega}(t) \end{pmatrix} = -\mathscr{R}(t) \cdot \mathscr{M}(t) \cdot \int_{S(t)} dS \begin{pmatrix} (\mathbf{n} \cdot \sigma_{\mathbf{T}})^T(t) \cdot \mathbf{u}'(t) \\ (\mathbf{n} \cdot \sigma_{\mathbf{R}})^T(t) \cdot \mathbf{u}'(t) \end{pmatrix} \tag{24}$$

$$= -\mathscr{R}(t) \cdot \mathscr{M}(g(t)) \cdot \int_{S(g(t))} dS \begin{pmatrix} (\mathbf{n} \cdot \sigma_{\mathbf{T}})^T(g(t)) \cdot \mathbf{u}'(g(t)) \\ (\mathbf{n} \cdot \sigma_{\mathbf{R}})^T(g(t)) \cdot \mathbf{u}'(g(t)) \end{pmatrix} \frac{dg(t)}{dt} \tag{25}$$

$$\begin{pmatrix} \mathbf{U}(t) \\ \mathbf{\Omega}(t) \end{pmatrix} = -\mathscr{R} \cdot \mathscr{R}^{-1}(g(t)) \cdot \begin{pmatrix} \mathbf{U}(g(t)) \\ \mathbf{\Omega}(g(t)) \end{pmatrix} \frac{dg(t)}{dt} \tag{26}$$

Using the fact that $\mathscr{M}(t) == \mathscr{M}(g(t))$, $S(t) = S(g(t))$, $\mathbf{\Sigma}_{T/R}(t) = \mathbf{\Sigma}_{T/R}(g(t))$. These hold as $\mathbf{f}(\mathbf{a}, t) = \mathbf{f}(\mathbf{a}, g(t))$

$$\mathbf{R}^{-1}(t) \cdot \mathbf{\Omega}(t) = \mathbf{R}^{-1}(g(t)) \cdot \mathbf{\Omega}(g(t)) \frac{dg(t)}{dt} \tag{27}$$

From 3, we get,

$$A_{ij}(t) = R_{li}^{-1} B_{lk} R kj = -\epsilon_{lkp} R_{li} R_{kj} \Omega_p \tag{28}$$

the from the determinant of the matrix R,

$$\epsilon_{lkp} R_{li} R_{kj} R_{pq} = |\mathbf{R}| \epsilon_{ijq}$$

Which in turn gives

$$\epsilon_{lkr} R_{li} R_{kj} = \epsilon_{ijq} R_{rq} = \epsilon_{ijq} (\mathbf{R}^{-1})_{qr}$$

Putting this back in 28,

$$A_{ij}(t) = -\epsilon_{ijk} (\mathbf{R}^{-1}(t) \cdot \mathbf{\Omega}(t))_k \tag{29}$$

29 and 27 together then give,

$$\mathbf{A}(t) = \mathbf{A}(g(t)) \frac{dg(t)}{dt} \tag{30}$$

The rotation matrix $\mathbf{R}(t)$ satisies the following relation

$$\frac{d\mathbf{R}(t)}{dt} = \mathbf{R}(t) \cdot \mathbf{A}(t) \tag{31}$$

Therefore,

$$\frac{d\mathbf{R}(g(t))}{dt} = \frac{dg(t)}{dt}\frac{d\mathbf{R}(g(t))}{dt} = \frac{dg(t)}{dt}\mathbf{R}(g(t)) \cdot \mathbf{A}(g(t)) = \mathbf{R}(g(t)) \cdot \mathbf{A}(t) \tag{32}$$

We also have, $\mathbf{R}(g(0)) = \mathbf{R}(0) = \mathbf{1}$ implying $\mathbf{R}(g(t)) = \mathbf{R}(t)$ thus $\mathbf{R}(g(T)) = \mathbf{R}(0) = \mathbf{1}$
Finally, consider,

$$\frac{d\mathbf{X}(g(t))}{dt} = \frac{dg(t)}{dt}\frac{d\mathbf{X}(g(t))}{dt} = \frac{dg(t)}{dt}\mathbf{U}(g(t)) = \mathbf{U}(t)$$

This taken together with $\mathbf{X}(g(0)) = \mathbf{X}(0)$ implies that $\mathbf{X}g(t) = \mathbf{X}(t)$ and thus,

$$\mathbf{X}(T) = \mathbf{X}(g(T)) = \mathbf{X}(0) = \mathbf{0} \tag{33}$$

This gives the proof for scallop theorem. A scallop or any such swimmer cannot swim in a low Reynolds number environment through reciprocal strokes.

When Can a Scallop Swim?

The scallop theorem tells us that swimmers at low Reynolds number cannot swim using reciprocal, i.e. time reversible swimming strokes. But in various settings a breakdown of the scallop theorem is observed. In this section we take a brief look at such places. Childress and Dudley (2004) noted that for a specific mollusc there were two ways of locomotion used, one was by the motion of cilia attached to its body by moving them in non-reciprocal strokes while the other was by using two *wings* which flapped in a reciprocal stroke. They were able to establish that there exists a transition at a critical value of flapping frequency when the frequency Reynolds number reaches a value of order unity. Looking at a spherical swimmer of radius a oscillatory surface deformations

$$Re_f = \frac{ad\omega}{\nu}$$

where, d is the amplitude of the oscillations, ω is the frequency, ν is the kinematic viscosity. Lauga (2007) was able to extend this analysis show that for any non zero value of Re_f the the scallop theorem breaks down with the effective induced velocity scaling as Re_f^{α}, $\alpha > 0$. Another recently observed effect was that of reciprocal strokes in non-Newtonian fluids.

Qiu et al. (2014) observed the motion of micro-scallops in a non-Newtonian environment using reciprocal swimming strokes. Mechanically constructed micro-scallops were made to execute a single hinge reciprocal motion in shear thinning as well as shear thickening environments. Net propulsion is observed when the speeds of opening and closing of the hinge

are different, with the best rate observed with faster closing speeds in shear thickening environments.

Keim et al. (2012) Observed similar results with reciprocal motions in a viscoelastic fluid surrounding. They submerged magnetic dimers in non-Newtonian surroundings and were able to make them perform reciprocal motions. They did so using two perpendicular magnetic fields, one for aligning the dimer and the other to perturb it from the state of alignment and thus cause oscillatory motions. They were able to observe net propulsion in the case of viscoelastic surroundings while no propulsion was observed in case of Newtonian fluid surroundings.

These examples of the breakdown of the scallop theorem lead us to discussions of a potential application of the same to study recently observed phenomena. The following section is dedicated to the same.

Potential for Application in a Non-biological System (Liquid Crystal)

The phenomenon discussed here is that of nucleation in liquid crystal systems during phase transition. Specifically the observations made recently at the soft matter lab at Ashoka University by Ankit Gupta and Dr. Pramoda Kumar. In case of a phase transition from the isotropic phase to the nematic phase nucleation was observed along with the growth of the droplets but after tracking the centre of mass of the droplets, it was seen that there was no net translation of the centre of mass of the droplets. At the phase transition form the nematic liquid crystal phase to the twist-bend nematic phase on the other hand, net translation of the centre of mass of the droplets was observed. In case of this phase transition, the nuclei again showed growth but along with this shape deformations of the droplets were also observed. The shape deformations were accompanied by the translation of the centre of mass of the droplets. The motion of the droplets was seen along the direction of the director.

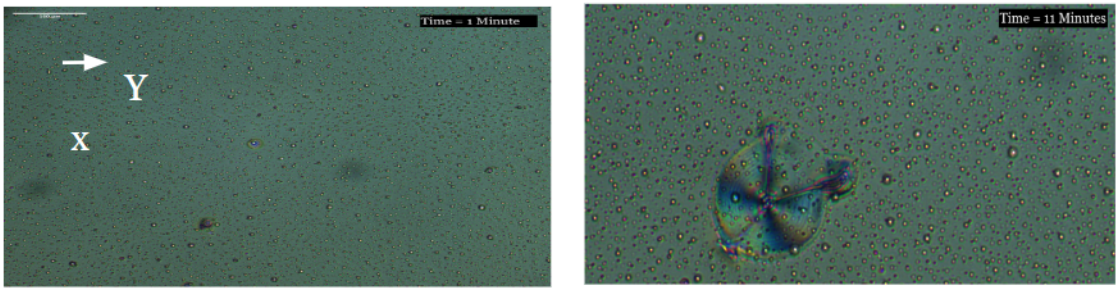

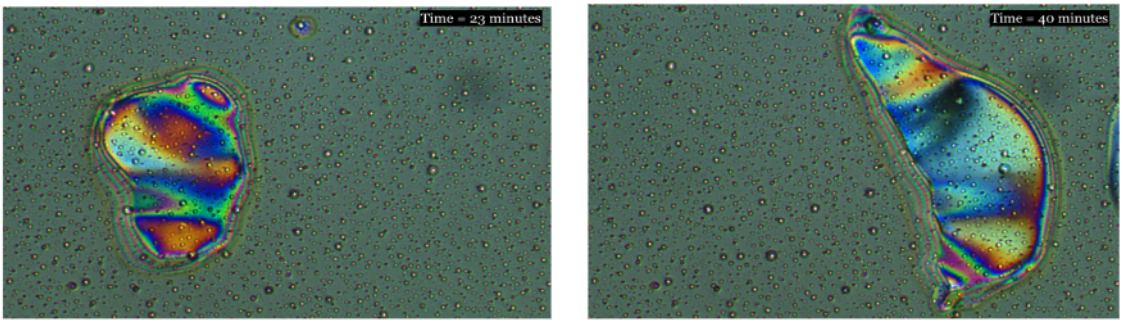

Figure 3: The growth and motion of Ntb droplet in a nematic surrounding (4/4). Image credit: Ankit Gupta, Ashoka University

Here I would like to put forth a candidate for an explanation for these experimentally observed phenomena. The translational motion accompanying the surface deformations and the absence of the same in case of the absence of the deformations is similar to the propulsion through surface deformations addressed in the preceding sections. The motion itself can readily be classified as low Reynolds number motion making this a possible candidate. We also note that the nematic liquid crystal environment in which the twist-bend nematic swimmer is present is a non-Newtonian, viscoelastic surrounding thus not only are non-reciprocal deformations a possible cause behind the translation but reciprocal deformations can also cause translational motion. The growth of the droplet itself is a sustained source of deformations leading to sustained motion of the droplets. It will be interesting to see the viability of this explanation but it looks to be a candidate worth looking at.

Acknowledgements

I would like to thank Professor Somendra Bhattacharjee for the for the opportunity to work on this project and his guidance. I would also like to thank Ankit Gupta and Dr. Pramoda Kumar for valuable discussions and observations from their experimental findings.

References

Childress, S., & Dudley, R. (2004). Transition from ciliary to flapping mode in a swimming mollusc: Flapping flight as a bifurcation in $Re\omega$. *Journal of Fluid Mechanics*, *498*, 257–288.

DeSimone, A., Alouges, F., & Lefebvre, A. (2008). Biological fluid dynamics: Swimming at low reynolds numbers. *Preprint*, (21).

Ishimoto, K., & Yamada, M. (2012). A coordinate-based proof of the scallop theorem. *SIAM Journal on Applied Mathematics*, *72*(5), 1686–1694.

Keim, N. C., Garcia, M., & Arratia, P. E. (2012). Fluid elasticity can enable propulsion at low reynolds number. *Physics of Fluids*, *24*(8).

Lauga, E. (2007). Continuous breakdown of purcell's scallop theorem with inertia. *Physics of Fluids*, *19*(6).

Morandotti, M. (2011). Self-propulsion in viscous fluids through shape deformation.

Purcell, E. M. (2014). Life at low reynolds number. In *Physics and our world: Reissue of the proceedings of a symposium in honor of victor f weisskopf* (pp. 47–67).

Qiu, T., Lee, T.-C., Mark, A. G., Morozov, K. I., Münster, R., Mierka, O., Turek, S., Leshansky, A. M., & Fischer, P. (2014). Swimming by reciprocal motion at low reynolds number. *Nature Communications*, *5*(1), 5119.

Shapere, A., & Wilczek, F. (1989). Geometry of self-propulsion at low reynolds number. *Journal of Fluid Mechanics*, *198*, 557–585.

Stone, H. A., & Samuel, A. D. (1996). Propulsion of microorganisms by surface distortions. *Physical Review Letters*, *77*(19), 4102.